Colloids and Surfaces B: Biointerfaces 159 (2017) 913–923

Contents lists available at ScienceDirect

Colloids and Surfaces B: Biointerfaces

journal homepage: www.elsevier.com/locate/colsurfb

COMPARATIVE PHYSIOCHEMICAL ANALYSIS OF HYDROPHOBINS PRODUCED IN *ESCHERICHIA COLI* AND *PICHIA PASTORIS*

Agnes Przylucka[a], Gunseli Bayram Akcapinar[a,*,1,4], Klaus Bonazza[b,2], Thiago M. Mello-de-Sousa[a], Astrid R. Mach-Aigner[a], Victor Lobanov[a], Hinrich Grothe[c], Christian P. Kubicek[a,d,3], Erik Reimhult[e,**], Irina S. Druzhinina[a,d,***,4]

[a] *Institute of Chemical, Environmental and Biological Engineering ICEBE, TU Wien, Gumpendorferstrasse 1a-ICEBE, 1060 Vienna, Austria*
[b] *Institute of Chemical Technologies and Analytics, TU Wien, Getreidemarkt 9/164-IAC,Vienna 1060, Austria*
[c] *Institute of Materials Chemistry, TU Wien, Getreidemarkt 9/165,Vienna 1060, Austria*
[d] *ACIB GmbH, c/o Institute of Chemical, Environmental and Biological Engineering ICEBE, TU Wien, Gumpendorferstrasse 1a-ICEBE,Vienna 1060, Austria*
[e] *Institute for Biologically Inspired Materials, Department of Nanobiotechnology, University of Natural Resources and Life Sciences, Muthgasse 11, Vienna 1190, Austria*

ARTICLE INFO

Article history:
Received 4 May 2017
Received in revised form 16 July 2017
Accepted 28 August 2017
Available online 4 September 2017

Keywords:
Atomic force microscopy (AFM)
circular dichroism (CD)
fungi
hydrophobin (HFB)
dynamic light scattering (DLS)
quartz crystal microbalance with dissipation monitoring (QCM-D)
recombinant protein production
small secreted cysteine rich proteins (SSCPs)
Trichoderma
water contact angle (WCA)

ABSTRACT

Hydrophobins (HFBs) are small surface-active proteins secreted by filamentous fungi. Being amphiphilic, they spontaneously form layers that convert surfaces from hydrophilic to hydrophobic and *vice versa*. We have compared properties of the class II HFB4 and HFB7 from *Trichoderma virens* as produced in *Escherichia coli* and *Pichia pastoris*. Since the production in *E. coli* required denaturation/renaturation steps because of inclusion bodies, this treatment was also applied to HFBs produced and secreted in yeast. The protein yields for both systems were similar. Both HFBs produced by *E. coli* proved less active on PET compared to HFBs produced in *P. pastoris*. HFBs produced in *E. coli* decreased the hydrophilicity of glass the most, which correlated with the adsorption of a more dense protein layer on glass compared to HFBs produced in *P. pastoris*. The hydrophobins produced in *P. pastoris* formed highly structured monolayers. Layers of hydrophobins produced in *E. coli* were less prone to self-organization. Our data suggests that irrespective of the production host, the HFBs could be used in various applications that are based on their surface activity. However, the production host and the subsequent purification procedure will influence the stability of HFB layers. In the area of high-value biomedical devices and nanomaterials, where the formation of highly ordered protein monolayers is essential, our results point to *P. pastoris* as the preferred production host. Furthermore, the choice of an appropriate hydrophobin for a given application appears to be equally important.

* Corresponding author at: Institute of Chemical, Environmental and Biological Engineering ICEBE, TU Wien, Gumpendorferstrasse 1a, Vienna 1060, Austria.
** Corresponding author at: Institute for Biologically Inspired Materials, Department of Nanobiotechnology, University of Natural Resources and Life Sciences, Muthgasse 11, Vienna 1190, Austria
*** Corresponding author at: ACIB GmbH, c/o Institute of Chemical, Environmental and Biological Engineering ICEBE, TU Wien, Gumpendorferstrasse 1a, Vienna 1060, Austria.
E-mail addresses: gunseli@sabanciuniv.edu (G.B. Akcapinar), erik.reimhult@boku.ac.at (E. Reimhult), irina.druzhinina@tuwien.ac.at (I.S. Druzhinina).
[1] Present address: Department of Statistics and Medical Informatics, School of Medicine, Acibadem University, Istanbul, Turkey.
[2] Present address: Program in Cellular and Molecular Medicine and Division of Hematology, Department of Medicine, Boston Children's Hospital, and Department of Biological Chemistry and Pharmacology, Harvard Medical School, Boston, MA, USA.
[3] Present address: Steinschötelgasse 7, Vienna1100, Austria.
[4] These authors contributed equally to the research.

http://dx.doi.org/10.1016/j.colsurfb.2017.08.058

1. INTRODUCTION

Fungal hydrophobins (HFBs) are extremely surface-active, small, secreted proteins. They are characterized by the conserved pattern of eight cysteine residues involved in four intramolecular disulfide bonds [1,2]. HFBs were initially categorized into two classes (I and II), based on differences in physical properties and hydropathic profiles [3], but recent data show that many HFBs do not fit into either group [4,5]. The characteristic property of HFBs is their ability to spontaneously self-assemble at hydrophobic–hydrophilic interfaces to form an amphipathic layer that converts the surface from hydrophilic to hydrophobic and *vice versa* [6–8].

The remarkable surface modulating activities of HFBs have been investigated for material coating [9–11], separation technologies [12,13], biosensors [14], production of cosmetics [15], and stabilization of foams in the food industry [16,17]. They are also attractive for medical applications as drug carriers [18] and as effectors that reduce implant rejection[19]. Finally, in some conditions, HFBs improve enzyme-catalysed polyester recycling [20,21].

The increasing demand for HFBs is faced with production challenges. In filamentous fungal hosts, produced HFBs remain largely bound to the hyphal cell wall, necessitating a further step in downstream processing [22,23]. While establishing the overproduction of the industrially interesting class II hydrophobins in *T. reesei*, the affinity to the cell wall was also observed (Przylucka, Lobanov, Druzhinina, unpublished data). Consequently, most authors used heterologous hosts – such as *Komagataella phaffii* (syn. *Pichia pastoris* [24]) or *Escherichia coli* – for HFB production [21,25–31]. An *E. coli*-based commercial recombinant production of HFBs as fusion proteins was developed by Wohlleben et al. [32].

The selection of which production host to use for recombinant HFB expression has so far been chosen rather arbitrarily, mainly based on the protein yield (Przylucka & Druzhinina, ms. submitted), but the possibility that different systems may influence the properties of the HFBs was not investigated. The objective of this work therefore was to compare the physicochemical properties of HFBs produced in two iconic expression systems, i.e. *E. coli* and *P. pastoris*. As model proteins, we have chosen two novel class II hydrophobins from *Trichoderma* – HFB4 [20,21] and HFB7 [33].

2. MATERIALS AND METHODS

2.1. Strains and Maintenance.

The sequences of *hfb4* and *hfb7* genes used in this study were taken from the genome of *T. virens* Gv 29-8 [34]; the strain is preserved in the TU Wien Collection of Industrial Microorganisms (TUCIM: 3530). The verification sequences have been deposited in Genbank under the numbers ABS59378 and ABS59373, respectively. The strain was cultivated on 3% malt extract (MEX) agar plates containing 100 mg/L chloramphenicol and 1.5% agar-agar (w/v) at 28 °C. *E. coli* Stellar™ Competent Cells (Takara Bio Company, CA, USA) were used for plasmid propagation and maintenance. The recombinant expression of HFBs was performed in *E. coli* BL21(DE3) strain (GE Healthcare, Amersham, England). Cultivation was performed in Lysogeny Broth (LB: 1% peptone, 1% sodium chloride, 0.5% yeast extract; all w/v) with 40 μg/ml kanamycin at 37 °C. *P. pastoris* strain KM71H (Life Technologies, CA, USA) and recombinant *P. pastoris* strains were maintained on yeast extract peptone dextrose (YPD: 1% yeast extract, 2% peptone, 2% dextrose; all w/v) agar plates containing 100 μg/ml Zeocin™ (Invitrogen) at 28 °C.

2.2. Plasmids and expression vectors

The primers given in Table S1 were used to amplify the cDNA fragments of *hfb4* and *hfb7*. Synthesis of cDNA has been described previously [33].

Digestion of DNA with restriction endonucleases (New England Biolabs, USA) and cloning with In-Fusion® HD Cloning (Takara Bio Company, CA, USA) were performed following the manufacturer's instructions. Pure Yield™ Plasmid Midiprep System (Promega) was used to isolate plasmid DNA, and their purification was performed using Qiagen DNA purification kits (Qiagen, Germany).

For expression in *E. coli*, the hydrophobin genes were fused between a 5′ *pelB* leader sequence and a 3′-sequence encoding a 6XHis Tag using the restriction sites *BamHI* and *XhoI* in the pET26b (+) (Novagen, Germany) vector. For recombinant expression in *P. pastoris*, the pPICZαA vector (Life Technologies, CA, USA) and restriction sites *EcoRI* and *XbaI* were used according to the manufacturers recommendations. pPICZαA and pET26b (+) plasmids were maintained in *E. coli* Stellar™ Competent Cells grown on low salt LB medium with 25 μg/ml Zeocin or 40 μg/ml Kanamycin, respectively.

2.3. Molecular biological techniques

The pET26b (+) vectors containing *hfb* genes were transformed to competent *E. coli* BL21(DE3) cells (New England BioLabs GmbH, Germany) with a heat shock at 42 °C for 45 sec. Positive clones were selected on LB plates containing 40 μg/ml kanamycin. The transformation of *P. pastoris* strain was performed according to the instructions of the manufacturer (Life Technologies, CA, USA). pPICZαA vectors containing HFB4 and HFB7 genes respectively were linearized using *Sac*I and transformed into the appropriate *P. pastoris* strain KM71H by electroporation. Transformants were grown on YPD agar plates with 100 μg/ml zeocin for selection of positive clones.

2.4. Production of HFB4 and HFB7

Cultivation conditions. All fermentations were performed in a 2 L BiostatA fermenter (Sartorius, Göttingen, Germany) with a working volume of 1 L.

Pichia pastoris. For high cell-density fermentation of recombinant *P. pastoris,* a fed-batch fermentation procedure was set up. A pre-culture was grown in YPD medium for 48 hours, and then was used (100 ml) as an inoculum for the fermenter. The fermentation medium consisted of basal salts medium (2% (v/v) H_3PO_4, 4% (w/v) glycerol, 100 mM K_2SO_4, 75 mM KOH, 60 mM $MgSO_4$-$7H_2O$, 7 mM $CaSO_4$). After 16 hours, a 50% glycerol (w/v) feed containing 12 ml/L trace salts (234 mM $FeSO_4$-$7H_2O$, 147 mM $ZnCl_2$, 24 mM $CuSO_4$-$5H_2O$, 18 mM $MnSO_4$- H_2O, 4 mM $CoCl_2$, 0.8 mM biotin, 0.8 mM Na_2MoO_4–$2H_2O$, 0.5 mM NaI, 0.3 mM H_3BO_3, 0.5% (v/v) H_2SO_4) was initiated. The expression was induced by a methanol feed (including 12 ml/L trace salts) after further 10 hours of fermentation. The temperature was kept at 28 °C constantly, and the pH maintained automatically at 5.0 using 25% (w/v) NH_4OH or H_3PO_4. Dissolved oxygen was kept above 30%.

Escherichia coli. The fermentation of HFB-producing *E. coli* was performed in a medium consisting of (conc. in mM) KH_2PO_4 (100), $(NH4)_2HPO_4$ (30), citric acid (10), glucose (167), $MgSO_4 \times 7H_2O$ (5), thiamine (0.015) and 40 μg/ml kanamycin. 10 ml/L of trace elements solution, pH 6.3, with Fe (III) citrate (40), $CoCl_2$-$6H_2O$ (1), $MnCl_2$-$4H_2O$ (8), $CuCl_2$-$2H_2O$ (0.9), H_3BO_3 (5), Na_2MoO_4-$2H_2O$ (1), Zn acetate-$2H_2O$ (6) and EDTA (3) was added. A pre-culture was grown overnight in 10 mL LB broth at 37 °C and 170 rpm. 10 ml fresh LB broth were inoculated with 100 μl of the overnight culture and cultivated for further 8 hours under the same conditions.

The final culture was then used to inoculate the fermenter. The pH was maintained at 6.8 with 5 M NaOH. The temperature was set to 37 °C for the biomass growth and subsequently lowered to 20 °C for the protein expression. Dissolved oxygen levels were kept above 30%. After 17 hours, a 0.389 M glucose feed (containing 64 mM $MgSO_4$, 2.00 ml of 100 x trace metal solution, 0.15 mM thiamine, 40 μg/ml kanamycin) of 5.8 ml/h was applied to boost the cell density. During the following eight hours, the feed was increased until 14.5 ml/h and kept at this rate for the induction phase. Eight hours later, the temperature was lowered to 20 °C and hydrophobin expression induced by the addition of 1 mM (final concentration) of isothiopropyl-β-D-galactoside (IPTG) in 0.14% (w/v) yeast extract.

2.5. Downstream processing: purification

HFBs were purified using the HisTALON™ Gravity Column Purification Kit (Takara Bio Company, CA, USA) as recommended for the solubilization of inclusion bodies by the manufacturer. An on-column refolding was performed using a step-wise gradient from 8 to 0 M urea using a washing buffer that contained additionally 1 mM reduced glutathione and 0.1 mM oxidized glutathione. For each step, two column volumes were used until the buffer was free of urea. Vivaspin ultrafiltration devices with 5 kDa cut-off (GE Healthcare, Amersham, England) were used for buffer exchange to 100 mM K_2HPO_4/KH_2PO_4 buffer at pH 6.6. The culture broth from *P. pastoris* was centrifuged at 936 g for 15 minutes to remove the cells. Urea was then added to a final concentration of 8 M and the samples purified the same way as described above over Co-charged affinity resin. Alternatively, the cell-free culture broth was filtered (pore size 0.22 μm, cellulose acetate membrane; Merck Millipore, Germany) and then subjected directly to the same buffer exchange.

2.6. Protein quantification

Protein concentration was determined using the BCA protein assay kit (Thermo Fisher Scientific GmbH, USA) and bovine serum album as standard according to the manufacturer's instructions.

2.7. Comparative characterization of HFB4 and HFB7

SDS-PAGE. Purified proteins and culture filtrates were analyzed on 15% SDS-polyacrylamide gels [35]. Silver and glycoprotein staining were performed using the SilverQuest™ Kit (Invitrogen, CA,USA) and the Pierce™ Glycoprotein Staining Kit (Thermo Fisher Scientific GmbH, USA), respectively.

Protein immunoblotting assay. Proteins, separated on 15% SDS PAGE gels as described above, were blotted onto 0.45 μm nitrocellulose membranes. Immunological visualization of HFB4 and HFB7 was performed using a mouse anti-his-tagHRP antibody. The target proteins were visualized following the protocol supplied with Clarity™ Western ECL. All products and devices were purchased from Biorad or Life Technologies.

Protein identification and glycopeptide analysis using LC-ESI-MS. Protein bands were cut out and digested in gel with sequencing grade modified trypsin (Promega) or sequencing grade chymotrypsin (Promega) after S-alkylation with iodoacetamide [36]. The peptide mixture was separated on a Dionex Ultimate 3000 system directly linked to a QTOF instrument (maXis 4G ETD, Bruker) equipped with the CaptiveSpray nanoBooster source in the positive ion, DDA mode (i.e. switching to MSMS mode for eluting peaks). MS-scans were recorded in the range of 150–2200 Da, and the six dominant peaks selected for fragmentation. Instrument calibration was performed using ESI calibration mixture (Agilent). For separation of the peptides a Thermo Acclaim PepMap RSLC C18 separation column (2 μm particle size, 100 Å, 250*0.075 mm) was used (with a Thermo Acclaim PepMap300 C18 μ-precolumn, 5 μm particle size, 300 Å Wide Pore, 5*0.3 mm). A gradient from 95% solvent A to 5% solvent B (Solvent A: 65 mM ammonium formiate buffer, B: 100% ACCN) to 32% B in 45 min was applied, followed by a 15 min gradient from 32% B to 80% B that facilitates elution of large peptides, at a flow rate of 0.3 μL/min. Data Analysis 4.0 (Bruker). The analysis files were converted to XML files, which are suitable to perform MS/MS ion searches with MASCOT (embedded in ProteinScape 3.0, Bruker) for protein identification, with the software Data Analysis 4.0 (Bruker). Only proteins identified with at least two peptides with a protein score higher than 80 were accepted. For the similarity searches, the SwissProt and NCBI databases were used.

For the measurement of the molecular weight, the proteins were directly injected to a LC-ESI-MS system (LC: Dionex Ultimate 3000 LC). A gradient from 10 to 80% acetonitrile in 0.05% trifluoroacetic acid (using a Thermo ProSwift™ RP-4H column (0.2 × 250 mm)) at a flow rate of 8 μL/min was applied. Detection was performed with a Q-TOF instrument (Bruker maXis 4G) equipped with the standard ESI source in positive ion, MS mode (range: 400–3000 Da). Instrument calibration was performed using ESI calibration mixture (Agilent). The data were processed using Data Analysis 4.0 (Bruker) and the spectrum was deconvoluted by MaxEnt.

Circular dichroism (CD) spectroscopy. Solutions of HFB4 and HFB7 (5 μM in 10 mM potassium phosphate pH 6.6) were used for CD spectroscopy measurements. Measurements were carried out in 0.2 cm SUPRASIL® quartz cells (Hellma Analytics, Müllheim, Germany) in a J-815 CD Spectrometer (Jasco, Tokio, Japan) at 20 °C. CD spectra of the proteins were collected from 260–190 nm as average of five scans and baseline subtracted in order to exclude buffer influences. Data are presented as the mean residue ellipticity [θ] in $deg \cdot cm^2 \cdot dmol^{-1}$, i.e. (millidegrees × MRW)/(pathlength in mm × concentration in mg/ml), where MRW is the mean residue weight. Secondary structure prediction was performed employing the analysis programme K2D3 [37] (http://cbdm-01.zdv.uni-mainz.de/~andrade/k2d3//index.html). CD spectra were plotted and analyzed to determine the folding state using a CD Analysis and Plotting Tool Capito [38] without further smoothing (http://capito.nmr.leibniz-fli.de/).

Structural models. Both HFB4 and HFB7 *T. virens* Gv 29-8 were homology modelled with Modeller9v2 [39] using the ultra-high resolution structure of the hydrophobin HFB2 from *T. reesei* (pdb ID: 2B97) as the modelling template. Secondary structure values were calculated from PDB files of the homology modelled proteins using StrucTools (https://hpcwebapps.cit.nih.gov/structbio/) for comparison with the secondary structure information obtained with CD spectroscopy.

Dynamic light scattering (DLS). The soluble-state of hydrophobins in distilled water (HPLC gradient quality; Carl Roth GmbH & Co, Germany) was measured in a Zetasizer (Malvern) at a concentration of 0.6 g/L. The samples were passed through a Whatman® Anotop® syringe filter (Sigma-Aldrich, USA) with a 0.2 μm pore size and shortly before the measurement centrifuged at 13 000 rpm for 30 min at 4 °C. The supernatant was used for the measurement at 25 °C. Fifteen spectra were recorded for each sample.

Water contact angle (WCA) measurement. The measurements were performed as described previously [20] using a Krüss Easy Drop DSA20E. Surfaces were prepared in three replicates and washed thoroughly before each measurement.

Atomic force microscopy (AFM). Protein layers were prepared and imaged as described previously [40]. Surfaces were rinsed before the measurement was performed.

Quartz crystal microbalance with dissipation monitoring (QCM-D). Quartz crystal sensors (4.95 MHz, AT-cut, gold electrode from LOT Quantum Design, Darmstadt, Germany), coated with a homogeneous film of either borosilicate or polyethylene terephthalate

(PET), were used. All measurements were conducted at 25 °C with a Q-Sense E4 (4 sensor system) system (Biolin Scientific, VästraFrölunda, Sweden). Each HFB was prepared in three biological replicates. At least five measurements were performed per HFB and expression system. The measurement cell was injected with a solution containing 5 μM hydrophobins until the surface was saturated. Thereafter, the stability of the adsorbed protein layer was tested by rinsing with potassium phosphate buffer for 30 minutes. The changes in resonance frequency (Δf) and energy dissipation (ΔD) after the deposition of hydrophobins on the surfaces were measured at 6 overtones (n = 3, 5, 7, 9, 11 and 13). The Q-Tools 3.1 software package (Biolin Scientific, VästraFrölunda, Sweden) was used to extract and normalize data.

3. RESULTS

3.1. Production of HFB4 and HFB7 in P. pastoris and E. coli cell factories results in similar protein yields

To produce HFB4 or HFB7 in *P. pastoris*, an inducible expression secretion system following a fed-batch strategy with a glycerol carbon source was used (*vide supra*). Thus, the *AOX1* promoter and the α-mating factor signal peptide were used for induction and secretion, respectively (Fig. S1 A). This resulted in the production of about 0.6 g/L of total extracellular protein with a total cell mass of 45 g/L, corresponding to a final specific production of 13.3 mg protein/g cell dry weight. The concentrations of $HFB4_{Pp}$ and $HFB7_{Pp}$ ("Pp" subscript for *P. pastoris*) in the broth were 6.9 and 8.1 mg/g of dry cell weight, respectively.

In *E. coli*, the inducible (*lacZ* promoter) intracellular production in following a fed-batch strategy (Fig. S1 B) resulted in a final cell density of 40 g/L. The HFBs were trapped in inclusion bodies. After solubilizing, renaturation and purification 1.9 mg $HFB4_{Ec}$ and 3.0 mg $HFB7_{Ec}$, respectively, could be obtained from one gram of biomass ("Ec" subscript for *E. coli*).

A calculation of the specific production rates during the induction periods (*P. pastoris:* 45 hours, *E. coli*: 13 hours) showed that they were in the same range (mg/g·h): $HFB4_{Pp}$ (0.14), $HFB7_{Pp}$ (0.23), $HFB4_{Ec}$ (0.15), $HFB7_{Ec}$ (0.18), Fig. S1.

The purified $HFB4_{Ec}$ and $HFB7_{Ec}$ and the *P. pastoris* culture filtrates with $HFB4_{Pp}$ and $HFB7_{Pp}$ were analyzed by SDS-PAGE (Fig. 1). At this stage, their identities were confirmed by immunoblotting using an antibody against the 6xHis Tag (further LC-MS verification *vide infra*). The HFBs were observed in their monomeric (12–13 kDa) as well as putative dimeric (20–25 kDa) forms. Both HFBs from the culture filtrate expressed by *P. pastoris* displayed dispersed bands between 12 and 13 kDa. In the *P. pastoris* culture filtrates, only small amounts of background protein were detected by silver staining. After purification, putative dimeric bands were also visible on the gels. We note that $HFB4_{Pp}$ and $HFB7_{Pp}$ were not glycosylated (Fig. S2). The high molecular weight band observed in the glycostain is likely an endogenous *P. pastoris* protein, because it was also secreted by the untransformed strain.

To check whether the proteins produced by *E. coli* and *P. pastoris* contained the correctly processed amino acid sequence, LC-ESI-MS analysis was performed. Although the sequence recovery was variable ($HFB4_{Pp}$ – 62.5%; $HFB7_{Pp}$ – 25.3%; $HFB4_{Ec}$ – 45.8%; and $HFB7_{Ec}$ – 75.4%; see Fig. S3 A), the sequences of the tryptic fragments perfectly matched those theoretically present in the mature hydrophobins. Only small amounts of common contaminations were detected [mainly trypsin and human keratin type I, [41]).

E. coli produced HFBs were located in inclusion bodies (*vide supra*). In order to check whether the on-column refolding indeed fully renatured the proteins, the oxidation state of the four disulfide bonds was investigated. The theoretical average mass of the mature hydrophobins with all disulfide bonds in their reduced state was calculated as 10659.13 Da and 9721.21 Da for $HFB4_{Ec}$ and $HFB7_{Ec}$, respectively. The actual protein mass measured in solution was 8 Da smaller than these values, thus proving that the eight hydrogen atoms were no longer present on the cysteine residues, and therefore four disulfide bonds had been formed (Fig. S3 B). The measured values of 10651.37 Da for $HFB4_{Ec}$ and 9713.59 Da for $HFB7_{Ec}$ correspond to the theoretical mass calculated for both monomeric hydrophobins with all eight cysteines in an oxidized state.

3.2. HFBs produced in P. pastoris and E. coli differ in secondary structure motifs

The 2D structure of class II hydrophobins typically consists of four β-sheets and a single α-helix [42,43]. We used far-UV CD spectroscopy to test whether the expression systems have an impact on HFB4 and HFB7 secondary structure after all necessary downstream processing steps. Generally, and irrespectively of the host used, the CD spectra of the HFB4 and HFB7 showed a maximum ellipticity close to 190 nm and a minimum around 200 nm. Specifically, $HFB4_{Ec}$ and $HFB7_{Ec}$ exhibited a minimum close to 204 and 203 nm, respectively (Fig. 2), which resembles the typical spectra of intrinsically disordered proteins [44]. This was further verified by the double wavelength analysis performed with CAPITO web server, where $[\theta]_{222}$ is plotted against $[\theta]_{200}$ to determine the folding state of each protein. The double wavelength plot of HFB4 revealed that its production in *E. coli* and *P. pastoris* both resulted in a pre-molten globule-like state in solution. Oxidative refolding steps during purification shifted $HFB4_{Pp}$ towards a native-like state. On the other hand, the double wavelength plot of HFB7 reveals different characteristics: as explained above, both $HFB7_{Ec}$ purified through denaturation and renaturation steps and $HFB7_{Pp}$ obtained from supernatant without purification exhibit pre-molten globule-like states. However, when $HFB7_{Pp}$ was purified through oxidative refolding steps, it was found in a coil-like state (Fig. 2). Overall, CD spectra recorded for both proteins, irrespective of the host, show high similarity to those of *T. reesei* HFB1 and HFB2 [23]. Nevertheless, a comparison of the CD spectra revealed major variations in the predicted secondary structures of the proteins (Table 1) compared to the theoretical secondary structure of HFB4 and HFB7. The percentage of α-helices was considerably lower than theoretically predicted (e.g. 2.92–4.01% vs. 13.7–11.7%), which is likely because the α-helices are only formed when hydrophobins bind to a solid surface [23,45]. On the other hand, the β-sheet content of HFB4 produced in either host match the theoretically calculated values after the purification and oxidative refolding steps. This is also valid for $HFB7_{Ec}$. Although oxidative refolding of $HFB7_{Pp}$ increased the β-sheet percentage, it was still lower than the theoretical values.

3.3. Aggregation of hydrophobins in solution is influenced by the expression system and varies between HFBs

We used DLS to estimate the aggregation behavior of HFB4 and HFB7 produced in the two expression systems. Volume-weighted size distributions are shown in Fig. 3. The clear majority of $HFB4_{Ec}$ displayed a hydrodynamic size of 8.3 ± 4.0 nm. However, a minority of the protein was also found in large aggregates with a size >5000 nm as seen in the intensity distribution (data not shown). The small fraction could correspond to monomers, dimers or small clusters. When the size of the structurally similar HFB1 (2–3 nm [42]) is used as a reference, this corresponds to the formation of dimers or small oligomers. $HFB4_{Pp}$ formed larger aggregates with a dynamic size of 105.6 ± 51.3 nm. However, when $HFB4_{Pp}$ was oxidatively refolded like $HFB4_{Ec,}$ it again displayed a small hydrodynamic size of 4.1 ± 0.2 nm, which could correspond to dimers or even monomers. A very small amount of the protein was also

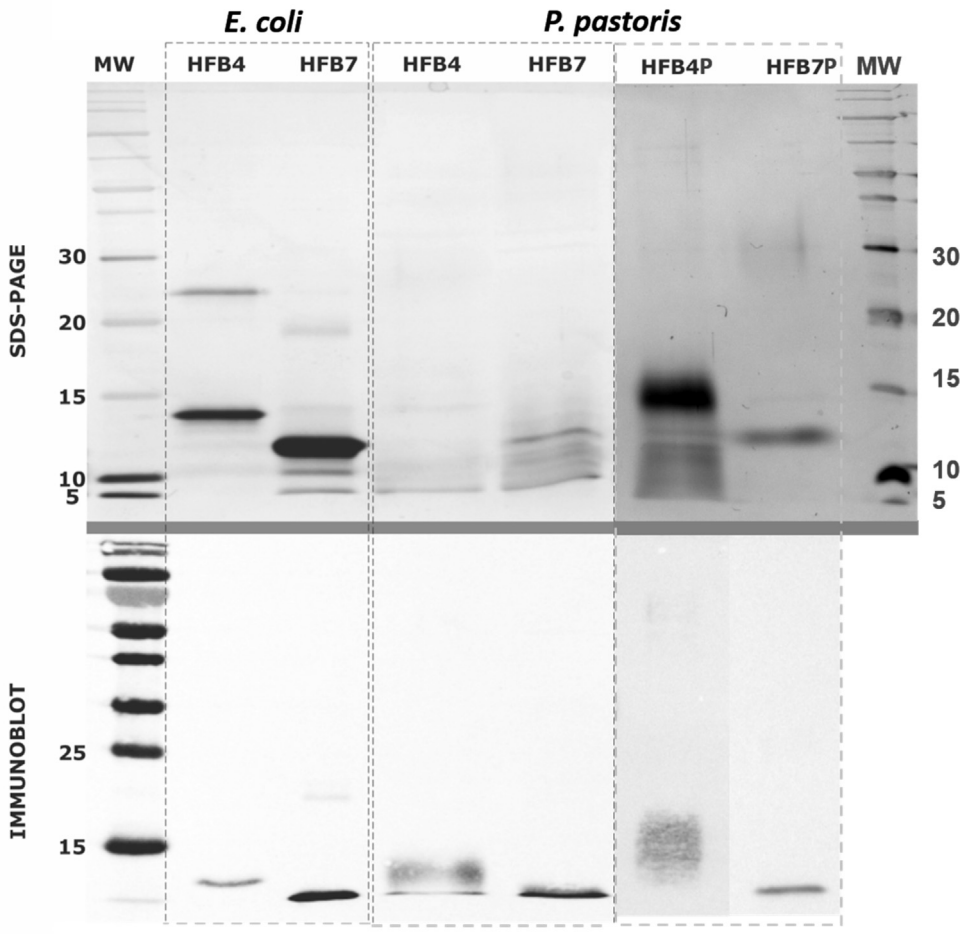

Fig. 1. Silver-stained SDS-PAGE (above) and immunoblot (below) of HFB4 and HFB7 produced in *E. coli* and *P. pastoris*. Hydrophobins produced in *E. coli* are shown after a purification and on column refolding step on IMAC. Culture broth after buffer exchange from *P. pastoris* is shown. HFB4P and HFB7P refer to hydrophobins produced in *P. pastoris* and purified including an oxidative refolding step. Molecular weight standards (MW) are given in kDa.

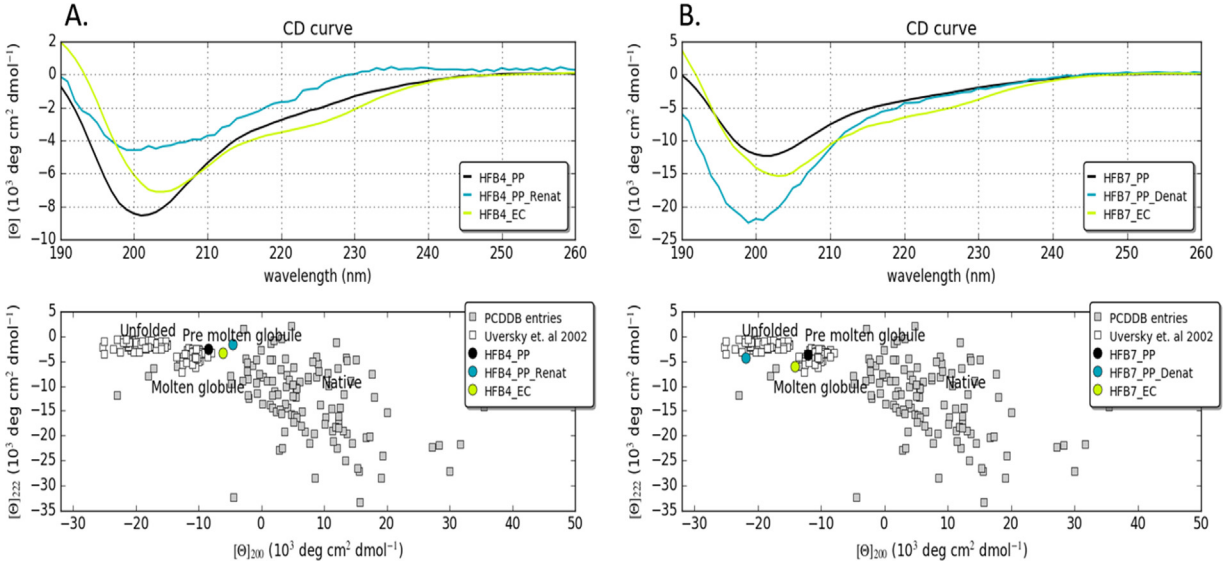

Fig. 2. Above: CD spectra of HFB4 (A) and HFB7 (B) produced in *P. pastoris* (black) and purified with an oxidative refolding step (blue) and *E. coli* (green). CD spectra are averages of five scans. Below: double wavelength analysis performed with CAPITO web server for the determination of the folding state of each protein.

here found in large aggregates with a size >100 nm in the intensity distribution (data not shown). $HFB7_{Ec}$ displayed a dynamic size of 7.5 ± 0.5 nm, while $HFB7_{Pp}$ formed aggregates of 58.8 ± 34.2 nm (70% of estimated protein mass) and 368.2 ± 174.7 nm (30% of estimated protein mass) respectively (Fig. 3B). Interestingly, $HFB7_{Pp}$ did not form aggregates after a refolding step, but displayed a size of

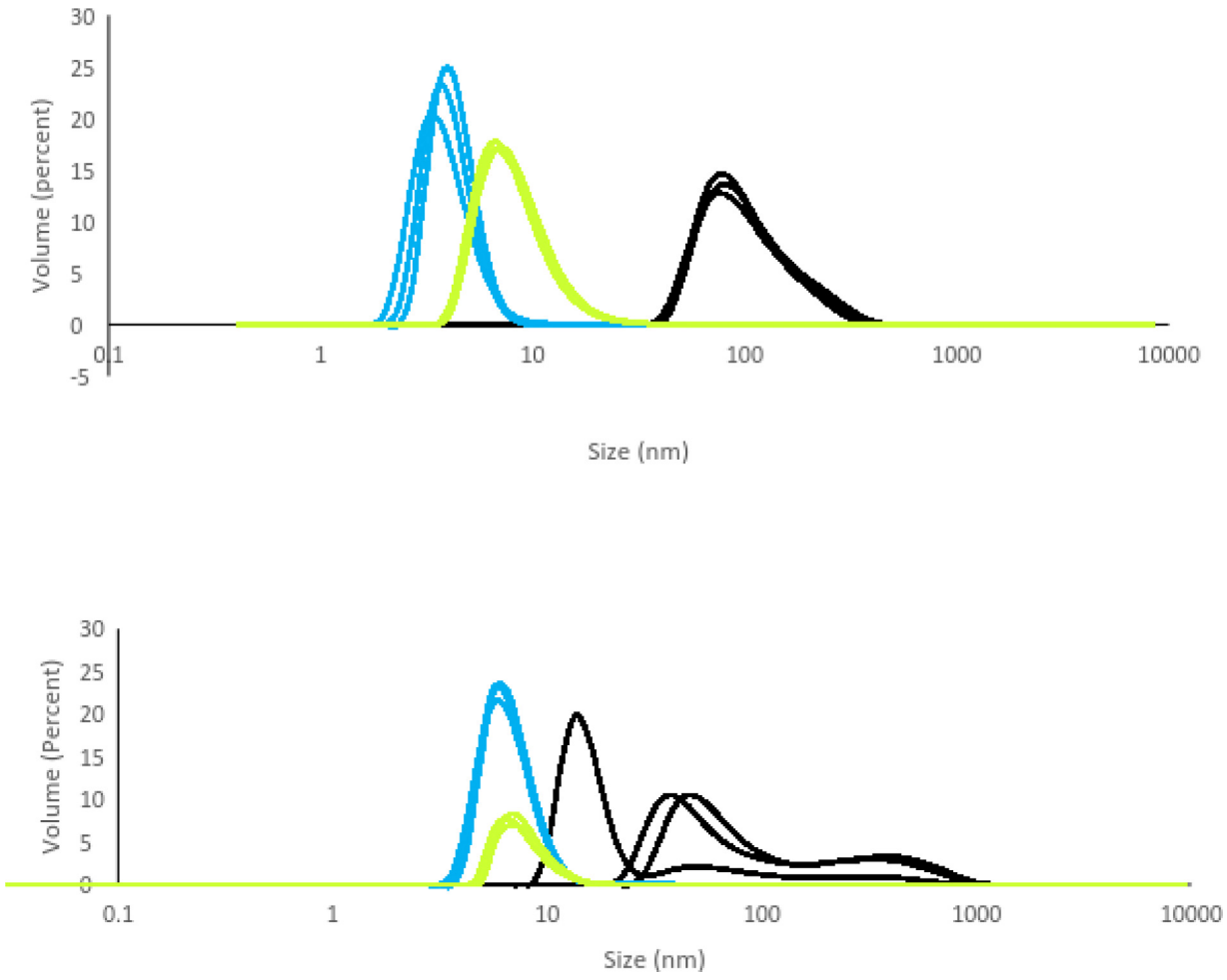

Fig. 3. Particle size distribution determined by mass measured by dynamic light scattering (DLS) for HFB4 (above) and HFB7 (below). Hydrophobins produced in *E. coli* are marked in green, in *P. pastoris* are marked in black and after purification with oxidative refolding in blue. Each line specifies results from a separate experiment.

around 6.6 ± 0.13 nm with only a minor aggregate presence around 400 nm.

3.4. *The surface modulation activity of individual HFBs is influenced by structural differences*

All HFB4 and HFB7 preparations could decrease hydrophobicity of PET, yet the proteins produced in *P. pastoris* were more effective in this regard (Table 2). $HFB4_{Pp}$ and $HFB7_{Pp}$ displayed no significant difference in their surface modulating activity neither in purified nor in non-purified form. The ability to render glass more hydrophobic was stronger for both HFB4 and HFB7 when produced in *E. coli* than when produced in *P. pastoris*. In particular, $HFB4_{Pp}$ had no surface modulating effect.

3.5. *HFBs expressed in* P. pastoris *form regular rows of dimers on a flat hydrophobic surface*

Investigations of HFB4 and HFB7 by atomic force microscopy (AFM) amplitude error images (Fig. 4) show far-distance ordered (crystalline) hydrophobin protein self-organization on a hydrophobic surface of highly ordered pyrolytic graphite (HOPG). $HFB4_{Pp}$ and $HFB7_{Pp}$ form regular rows with a separation of about 5.8 ± 0.2 and 6.5 ± 0.8 nm, respectively. Assuming a monomeric size of 2–3 nm (*vide supra*), the above values correspond to a HFB dimer (double rows). Patches of unidirectional rows are typically some 100 nm long and surrounded by narrow "grain boundaries". In some cases, also smaller disordered patches can be observed between the "grains". The "blobs", which can be seen in the images, are most probably due to an excess of hydrophobin that was not fully rinsed off. They appear to overlay the crystalline film as they do not interrupt the underlying rows. $HFB4_{Ec}$ shows a two-phase system with some crystalline regions and large disordered regions. In the crystalline regions, the lattice parameter is ~5.7 ± 0.2 nm. $HFB7_{Ec}$ also shows two phases, both of which are crystalline but clearly differ by the periodicities of rows that are either 7.3 ± 0.8 nm or 3.4 ± 0.5 nm. Moreover, a more frequent formation of grain boundaries, including more "blobs" compared to hydrophobins expressed in *P. pastoris*, can be observed.

3.6. *HFBs expressed in* E. coli *form more rigid films on both hydrophilic and hydrophobic surfaces compared to HFBs expressed in* P. pastoris

Typical kinetic traces for the hydrophobin adsorption recorded using QCM-D is shown in Fig. 5A and 5B. The displayed decrease in frequency is roughly proportional to an increase in adsorbed HFB layer mass including trapped water according to the Sauerbrey formular $\Delta m = -k\Delta f$, where $k \approx 18\ ng/cm^{-2}\cdot Hz$. Both HFBs adsorbed to both borosilicate and PET crystals to form layers of different mass that correspond approximately to monolayers of the protein (Fig. 5). While HFBs expressed in *E. coli* bind more mass to hydrophilic borosilicate, renatured hydrophobins expressed in *P. pastoris* bound very similar

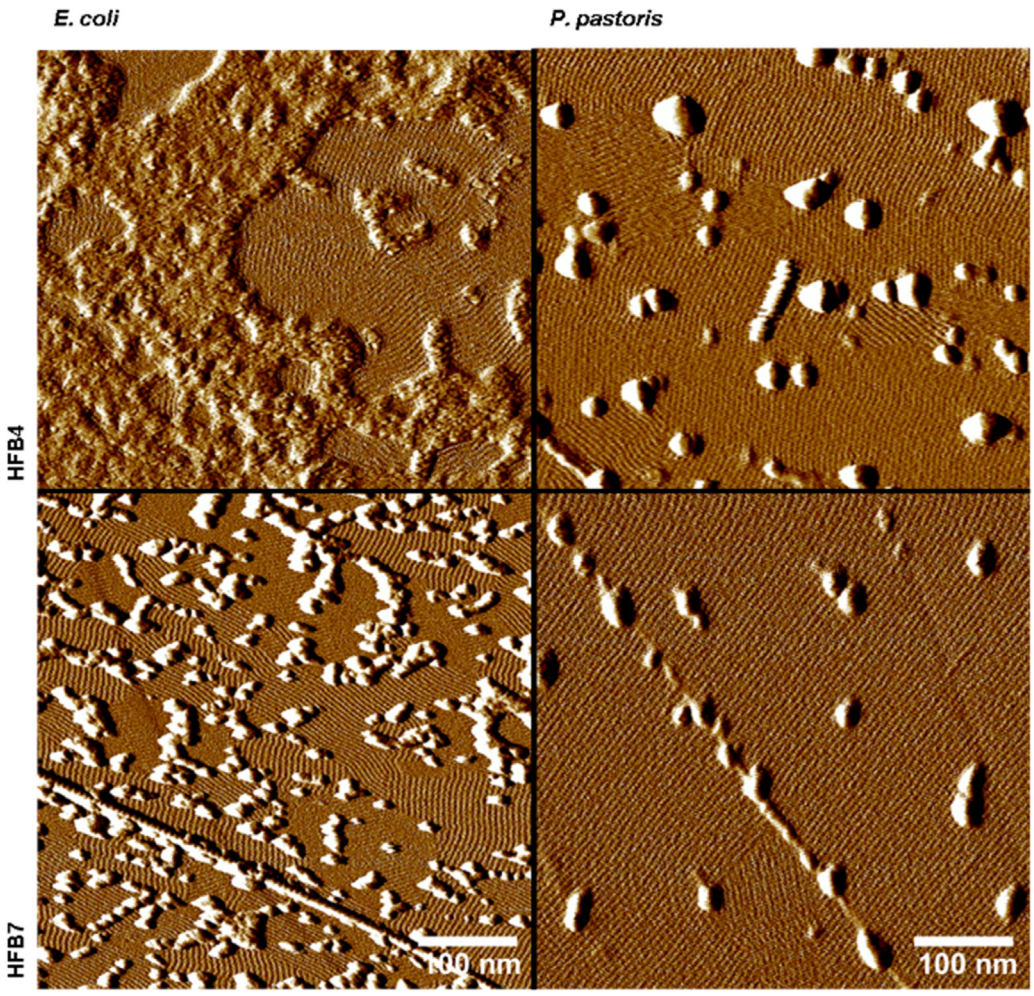

Fig. 4. Tapping mode atomic force microscopy amplitude error images of surface layers formed by HFB4 and HFB7 expressed in *E. coli* and *P. pastoris* cell factories.

amounts of protein to both types of surfaces (Fig. 5): $HFB7_{Ec}$ bound 480.4 ± 55.8 ng/cm^2 to PET and 777.0 ± 19.9 ng/cm^2 to glass before rinsing, whereas $HFB7_{Pp}$ deposited 637.7 ± 26.2 ng/cm^2 on PET and only 362.5 ± 60.7 ng/cm^2 on glass. After the renaturation step, $HFB7_{Pp}$ bound 491.76 ± 25.63 ng/cm^2 on PET and 521.64 ± 27.95 ng/cm^2 on glass, showing a very small decrease in surface coverage on PET compared to on glass.

$HFB4_{Ec}$ bound to PET at 625.5 ± 66.7 ng/cm^2 and to glass at 747.0 ± 44.0 ng/cm^2, while $HFB4_{Pp}$ adsorbed at 481.7 ± 73.3 ng/cm^2 to PET and initially at 574.5 ± 71.9 ng/cm^2 to glass. After the rinsing step, the mass of $HFB4_{Pp}$ bound to glass was reduced to 324.0 ng/cm^2 revealing a large fraction of weakly bound hydrophobin to the hydrophilic surface. Renatured $HFB4_{Pp}$ bound 547.38 ± 22.52 ng/cm^2 on PET and $588.24 \pm 8{,}44$ ng/cm^2 on glass, thus displaying similar mass deposition as the untreated $HFB4_{Pp}$. Renatured $HFB4_{Pp}$ was more easily removed from the surface during washing, a phenomenon particularly pronounced when using a glass surface.

The significant difference in the mass of the adsorbed layer before and after rinsing signifies that loosely bound $HFB4_{Pp}$ are present on the presumed HFB monolayer when a large excess of $HFB4_{Pp}$ is present in solution. $HFB7_{Ec}$ binds more mass than $HFB7_{Pp}$ to glass, but $HFB7_{Pp}$ binds more mass than $HFB7_{Ec}$ to PET. These differences are constant before and after rinsing. That is, rinsing does not lead to significant mass loss for any substrate version of HFB7.

4. DISCUSSION

In this study, we investigated whether the expression of two class II hydrophobins from the ascomycete *T. virens* – HFB4 and HFB7–in two canonical production systems for heterologous eukaryotic proteins, i.e. *E. coli* and *P. pastoris*, result in proteins with similar properties. Both systems have already been used for class I and II hydrophobin production before [21,25,27–32] but the properties of resulting proteins were not compared. Both HFB4 and HFB7 were produced in similar quantities and specific concentrations (mg/g host biomass). Hydrophobins from *P. pastoris* were displayed in multiple dispersed bands around 10 kDa on SDS-polyacrylamide gels. Since the form with the highest molecular weight matches that of the protein produced in *E. coli*, we propose that the additional forms are due to posttranslational processing. Similar modifications have been shown to occur both at the N- as well as C-terminal ends of hydrophobins of *T. reesei* [46] and *T. atroviride* [47].

Despite the use of a *pelB* leader sequence for secretion to the periplasmic space in the expression vector for *E. coli*, both HFB4 and HFB7 were still concentrated in inclusion bodies. The leader sequence was not present in mature proteins, indicating that they had indeed been translocated to the periplasmic space. However, the formation of inclusion bodies in the periplasma has been reported previously [48]. Therefore, it was necessary to purify the proteins under denaturing conditions and subsequently refold them. The determination of molecular weight of the final protein product using mass spectrometry showed that all eight cysteines

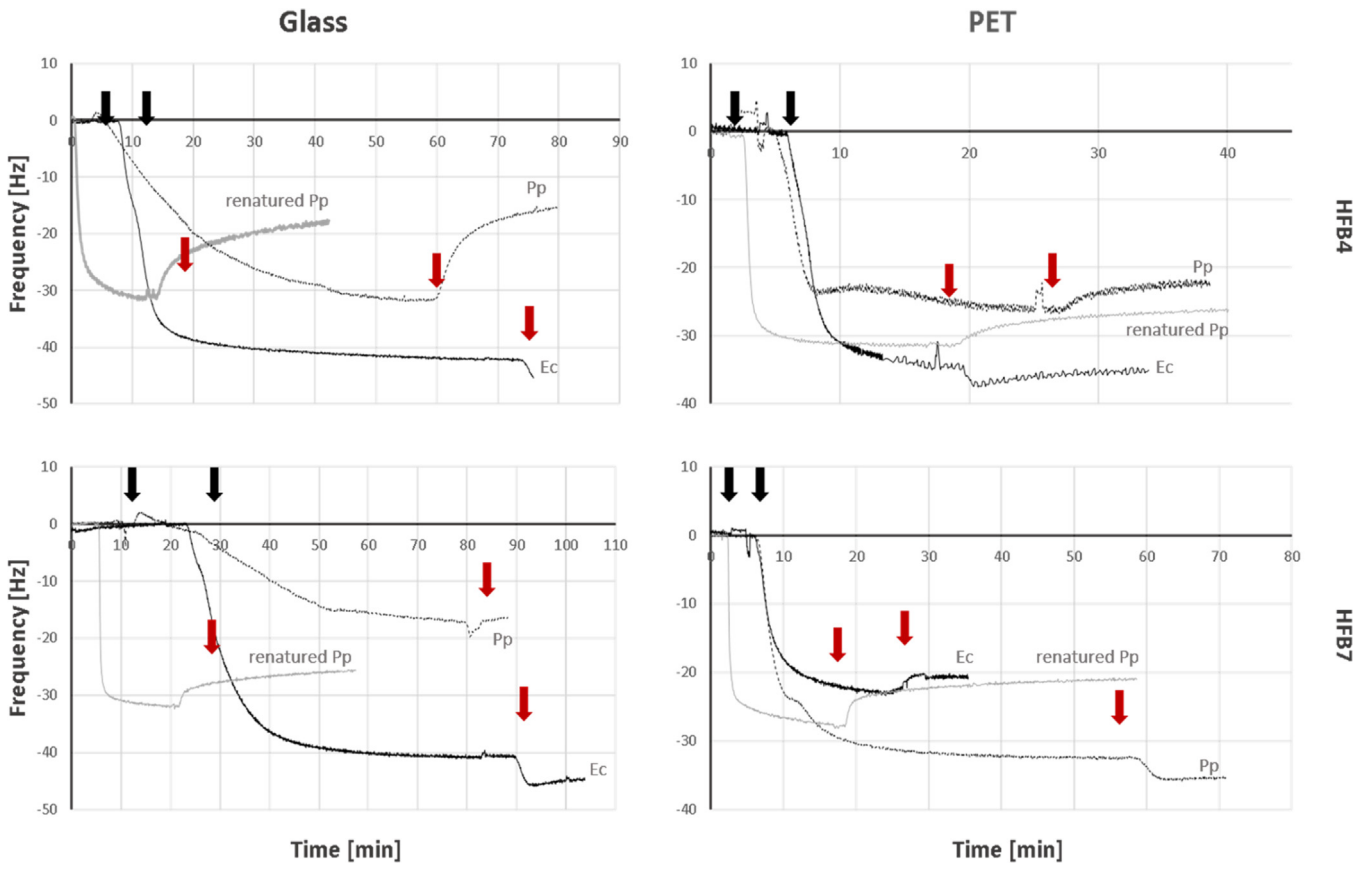

Fig. 5. Representative adsorption kinetics recorded using quartz crystal microbalance for the interaction of all hydrophobin variants with borosilicate (left) and PET (right) substrates. HFB4 is shown in the top row and HFB7 in the bottom row. Frequency changes are shown for the 3rd overtone normalized to the fundamental resonance frequency. Black and red arrows indicate the sample application and start of the buffer rinse, respectively. Hydrophobins produced in *E. coli* are shown in black, in *P. pastoris* in dashed (native) and grey (renatured) line.

were in a fully oxidized state. We should note, however, that this does not rule out that they may have formed S-S bridges in a different way from that in the native protein. In order to make a direct comparison of hydrophobins derived from both expression system, both $HFB4_{Pp}$ and $HFB7_{Pp}$ were purified analogously. However, $HFB4_{Pp}$ and $HFB7_{Pp}$ were also directly subjected to the analysis pipeline after buffer exchange of the culture filtrates, since qualitative analysis on SDS-PAGE showed that the proteins were secreted with little protein background in the culture filtrate and thus would be the most suitable for applications.

We tested how the differences in downstream processing would influence the secondary structure and function of HFB4 and HFB7. The structural features were characterized by CD spectroscopy and showed protein-specific effects: $HFB4_{Ec}$, refolded $HFB4_{Pp}$, $HBF7_{Ec}$ displayed a β-sheet percentage that comes close to the theoretical value, suggesting that most of the β-sheets have been formed. In contrast, a much lower percentage of β-sheets was detected for renatured $HFB7_{Pp}$. It should be noted, however, that secondary structure predictions from CD spectra in the case of hydrophobins are prone to errors because the secondary structures are extrapolated from CD spectra based on known 3D structures in the database. As only a few hydrophobin structures have so far been resolved, and due to the intrinsically disordered β-sheet regions of the hydrophobins, these predictions may not fully reflect the actual situation. This could only be shown by X-ray crystallography or nuclear magnetic resonance spectroscopy. CD analysis by the CAPITO web server revealed that oxidative refolding of $HFB7_{Pp}$ resulted in a coil-like, unfolded state whereas all other forms of HFB4 and HFB7 were largely disordered and occurred in a pre-molten globule like-state. Proteins in the native pre-molten globule state are known to be more compact than random coils and exhibit ordered secondary structures that can be detected by far-UV CD spectroscopy to some extent. Their CD spectrum is characterized by having a minimal ellipticity in the vicinity of 200 nm, which is typical for disordered protein chains and is also valid for HFBs produced in both hosts. Additionally, we have observed different CD signal intensities at the same protein concentrations, which could be due to differences in protein aggregation tendencies. DLS data indicates that indeed aggregates were present. Moreover, the DLS data indicate that *P. pastoris* produced proteins are more prone to aggregation before the denaturation-oxidative refolding step. Disordered proteins would be more prone to large-scale aggregation, which supports the hypothesis that the refolding step produces HFBs closer to their natural fold and stability. While the oxidative refolding step has an impact on aggregation and protein structure, it had a minor effect on the surface activity of HFB4. On the other hand, as QCM measurements indicate, surface activity of HFB7 is affected more depending on if it is refolded or not. de Vocht et al. [50] have shown that disulfide bridges of *Schizophyllum commune* hydrophobin SC3 (Class I) were not directly involved in the self-assembly but were instead required to keep the monomeric state inside the cells or aqueous environments. Pronounced surface modulation activities were observed on both hydrophilic as well as hydrophobic surfaces. Both HFBs produced by *E. coli* proved much less active on PET than those HFBs produced by *P. pastoris.* We assume that this could be related to the formation of highly-oriented surface layer in HFBs produced by *P. pastoris*, while those produced in *E. coli* showed large unstructured areas (HFB4) or depo-

sition of aggregates (HFB7). The HFBs produced in *E. coli* decreased the hydrophilicity of glass more strongly, which also correlates with the binding of more mass of $HFB4_{Ec}$ and $HFB7_{Ec}$ to glass in QCM analysis.

The structures of hydrophobin layers revealed by AFM on the hydrophobic HOPG material show that the hydrophobins produced in *P. pastoris* formed highly structured layers with long-distance order. Hydrophobins produced in *E. coli* produced showed less self-organization in adsorbed surface layers. $HFB4_{Ec}$ formed mostly unstructured protein layers on the hydrophobic surface infused with small patches of ordered formation with similar lattice parameters as $HFB4_{Pp}$. Here, no deposition of large aggregates was observed, which also correlates to the finding that $HFB4_{Ec}$ occurs mainly in dimers in solution and does not form large aggregates. During binding to the HOPG surface, $HFB7_{Ec}$ layers also differed from the regular formation made by hydrophobins expressed in *P. pastoris*. Two different lattice parameters are observed. Probably the geometrical match is not perfect and hence the formation of large ordered layers of double rows as seen in $HFB4_{Pp}$, $HFB7_{Pp}$ and in the non-class II hydrophobin HFB9 [40] would result in mechanical stress. This could be reduced either by a different organization (the double row 7.3 nm distance does not match two single row 3.4 nm distances) or by frequent directional change. Also, depositions of large protein aggregates were more frequent on $HFB7_{Ec}$ layers compared to $HFB7_{Pp}$ layers. The hydrophobin layers observed by AFM showed great differences in structural organization and matched the surface activity observed on the hydrophobic substrate PET.

DLS, and especially AFM data, suggest that HFBs subjected to denaturation and subsequent refolding have two coexisting phases: fractions of large and small aggregates in DLS and differently organized regions in AFM. A potential explanation is that a different recombination of cysteins results in two different, coexisting disulfide patterns. HFBs consist of a stable and rigid barrel-shaped backbone of four β-strands and a charged α-helix that might only be stabilized in the surface bound state [42,43]. According to the crystal structures of HFB1 and HFB2, two disulfide bridges (C3-C4 and C7-C8 counting cysteins form the N-terminus) only connect neighboring β-strands and, thus, we think they are not essential for correct folding, explaining observations that disulfides may not be required for self-assembly although they are the only highly conserved feature of HFBs. Given the geometry of the rigid backbone, C2 is virtually impossible to combine with C6. Therefore, only two different S-S crosslinking patterns may be expected: Pattern 1 (C1-C6, C2-C5, C3-C4, C7-C8) which results from the published crystal structures and pattern 2 (C1-C2, C3-C4, C5-C6, C7-C8) [50]. We find it probable that HFBs secreted into the medium by *Pichia pastoris* show strictly pattern 1, whereas a refolding process allows for an equilibrium between patterns 1 and 2 resulting in two phases. The effect of swapping C1-C6, C2-C5 to C1-C2, C5-C6 is putatively minor in terms of 3-D structure and surface electrostatics but may destabilize the α-helix by pulling it towards C2. This is plausible only assuming the α-helix is formed in solution. While this feature exists in a NMR structure of the structurally similar chimeric hydrophobin NChi2 [51], it has been proposed that it may only form on surfaces. Our AFM data may give a first hint in resolving these contradictions. If HFBs with crosslinking pattern 1 would form the α-helix in solution, and crosslinking pattern 2 would require the surface to stabilize the helix, then in solution the pattern 1 HFBs represent more on-pathway intermediates towards the surface bound state whereas pattern 2 HFBs would require a conformational change during self-assembly. Indeed, only self-assembled surface structures of refolded HFBs, which may contain pattern 2, show signs of mechanical stress. It will be interesting to prove this model with solution structures of HFBs with different disulfide patterns.

QCM-D analysis has become a powerful analytical method for the interaction of microorganisms or biomolecules with surfaces [52,53] and was here used to illuminate variations in total amount of adsorbed protein and qualitative differences in the adsorptions kinetics. The deposited mass on glass was clearly higher for hydrophobins expressed in *E. coli*. The high density of adsorbed of both HFB expressed in *E. coli* correlates with a strong change in the wettability of glass rendering it more hydrophobic. HFB7 had a particular strong effect on the hydrophilic surface by changing its WCA from 12° to 62°. Also, even though $HFB4_{Pp}$ and $HFB7_{Pp}$ had a similar lower mass deposition on glass, $HFB7_{Pp}$ still showed a rather high surface modulating activity resulting in a WCA of 43°, while $HFB4_{Pp}$ did not produce a measurable change in the wettability of hydrophilic glass. Also this observation correlates with the QCM data as a large fraction of $HFB4_{Pp}$ is removed from the surface of glass, but not from PET after rinsing, additionally demonstrating a looser association with the hydrophilic surface. Thus, the negligible change in WCA is likely due to a low surface coverage of $HFB4_{Pp}$ on glass after rinsing and reorganization of the loosely bound protein at the interface during the contact angle measurement. The QCM data of the *E. coli* film indicate the formation of protein layers with high stability upon rinsing. There are notable differences in the adsorption kinetics on glass between the native and renatured HFBs expressed in *P. pastoris*. The native protein adsorbs much more slowly and the adsorption kinetics suggests that a defined monolayer might not be formed, but rather that slow continuous aggregation might occur on the surface. The renatured protein on the other hand, displays well-defined fast adsorption and formation of a stable monolayer. The slower and more ill-defined adsorption is likely due to slower mass transport of the native HFB_{Pp}, due to the prevalence of large aggregates of the native protein (*cf.* Fig. 3). Aggregates have lower mobility and adsorb to the surface at a lower rate for the same protein concentration as the measurements are performed under diffusion controlled kinetics conditions. However, it cannot be ruled out that additionally a more ill-defined protein conformation of the native HFB_{Pp} yields a weaker interaction with the hydrophilic surface. It should also be noted that when reversible adsorption is observed after rinsing, the renatured HFB_{Pp} show a fast and well-defined desorption. Thus, a larger fraction of the protein binds without denaturation to the interface and is in equilibrium with the bulk protein concentration. Interestingly, the HFBs expressed in *E. coli* on all surfaces showed higher stability to rinsing than HFBs expressed in *P. pastoris*, despite that the differences before rinsing between HFBs expressed in *E. coli* and renatured HFBs expressed in *P. pastoris* were minor. This difference in desorption kinetics was most pronounced for HFB4 on glass. Irreversible protein adsorption on solid surfaces is generally associated with either surface-induced partial denaturation or stabilizing protein-protein interactions. This indicate that the renatured HFBs from *P. pastoris* show higher structural stability and less formation of strongly associated dimers and oligomers on the surface than what is the case for HFBs expressed in *E. coli*. DLS also shows formation of oligomers of HFB4 already in solution, which correlates with the observation regarding the adsorbed protein layer stability.

We demonstrated that class II hydrophobins produced in two canonical hosts differ strongly in their surface modulating activities at hydrophilic and hydrophobic interfaces. Although all hydrophobins produced displayed the typical characteristics of adsorption and even partial self-organization as protein monolayers at interfaces, the affinity for hydrophilic versus hydrophobic surfaces showed significant variation. The differences in the stability and organization of self-assembled protein layers were not only HFB-specific but also production-host specific and the resulting structural features that varied due to the differences in downstream processing. Both HFBs expressed in *P. pastoris* required renaturing to achieve a native-like fold and avoid aggregation. The lack of

structure and presence of aggregates prevented rapid and defined surface assembly in particular on glass, leading to lack of surface modulation. Our data suggests that HFBs could be used in the various applications such as immobilization of enzymes for biosensors [54–60] irrespective of the production host, based on their surface activity. Stability, however, would depend also on the production host and subsequent purification method selected. Nonetheless, in the area of high-value biomedical devices and nanomaterials where the formation of highly-ordered protein monolayers is essential for a successful application, results of AFM-resolved structures would indicate that *Pichia pastoris* is the more appropriate host.

CONFLICT OF INTEREST

DISCLOSURE

The authors declare no competing financial interest.

ACKNOWLEDGMENTS

This study was partially supported by the Federal Ministry of Economy, Family, and Youth, the Federal Ministry of Traffic, Innovation, and Technology, the Styrian Business Promotion Agency, the Standortagentur Tirol, and the ZIT–Technology Agency of the City of Vienna through the COMET-Funding Program managed by the Austrian Research Promotion Agency FFG. ISD and AP were supported by the Austrian Research Fund (FWF) grants P25613 and P25745 to ISD. HG was supported by the Austrian Research Fund (FWF) grant P26040. CD spectroscopy was supported by an Innovative Project (RAKI-MINT) granted by TU Wien to ARMA.

Appendix A. Supplementary data

Supplementary data associated with this article can be found, in the online version, at http://dx.doi.org/10.1016/j.colsurfb.2017.08.058.

References

[1] A.H. Kwan, I. Macindoe, P.V. Vukašin, V.K. Morris, I. Kass, R. Gupte, A.E. Mark, M.D. Templeton, J.P. Mackay, M. Sunde, The Cys3-Cys4 Loop of the Hydrophobin EAS Is Not Required for Rodlet Formation and Surface Activity, J. Mol. Biol. 382 (2008) 708–720, http://dx.doi.org/10.1016/j.jmb.2008.07.034.
[2] M.B. Linder, Hydrophobins Proteins that self assemble at interfaces, Current Opinion in Colloid & Interface Science 14 (2009) 356–363, http://dx.doi.org/10.1016/j.cocis.2009.04.001.
[3] H.A. Wösten, F.H. Schuren, J.G. Wessels, Interfacial self-assembly of a hydrophobin into an amphipathic protein membrane mediates fungal attachment to hydrophobic surfaces, EMBO J. 13 (1994) 5848–5854.
[4] B.G. Jensen, M.R. Andersen, M.H. Pedersen, J.C. Frisvad, I. Søndergaard, Hydrophobins from *Aspergillus* species cannot be clearly divided into two classes, BMC Res Notes. 3 (2010) 344, http://dx.doi.org/10.1186/1756-0500-3-344.
[5] V. Seidl-Seiboth, S. Gruber, U. Sezerman, T. Schwecke, A. Albayrak, T. Neuhof, H. von Döhren, S.E. Baker, C.P. Kubicek, Novel Hydrophobins from *Trichoderma* Define a New Hydrophobin Subclass: Protein Properties, Evolution, Regulation and Processing, J. Mol. Evol. 72 (2011) 339–351, http://dx.doi.org/10.1007/s00239-011-9438-3.
[6] M. Sunde, A.H.Y. Kwan, M.D. Templeton, R.E. Beever, J.P. Mackay, Structural analysis of hydrophobins, Micron. 39 (2008) 773–784, http://dx.doi.org/10.1016/j.micron.2007.08.003.
[7] E.S. Basheva, P.A. Kralchevsky, N.C. Christov, K.D. Danov, S.D. Stoyanov, T.B.J. Blijdenstein, H.J. Kim, E.G. Pelan, A. Lips, Unique properties of bubbles and foam films stabilized by HFBII hydrophobin, Langmuir 27 (2011) 2382–2392, http://dx.doi.org/10.1021/la104726w.
[8] M.B. Linder, Hydrophobins: the protein-amphiphiles of filamentous fungi, FEMS Microbiol, Rev. 29 (2005) 877–896, http://dx.doi.org/10.1016/j.femsre.2005.01.004.
[9] S. Hou, X. Li, X. Li, X. Feng, Coating of hydrophobins on three-dimensional electrospun poly(lactic-co-glycolic acid) scaffolds for cell adhesion, Biofabrication. 1 (2009) 035004, http://dx.doi.org/10.1088/1758-5082/1/3/035004.
[10] H. Asakawa, S. Tahara, M. Nakamichi, K. Takehara, S. Ikeno, M.B. Linder, T. Haruyama, The Amphiphilic Protein HFBII as a Genetically Taggable Molecular Carrier for the Formation of a Self-Organized Functional Protein Layer on a Solid Surface, Langmuir 25 (2009) 8841–8844, http://dx.doi.org/10.1021/la900974n.
[11] M. Qin, L. Wang, X. Feng, Y. Yang, R. Wang, C. Wang, L. Yu, B. Shao, M. Qiao, Bioactive Surface Modification of Mica and Poly (dimethylsiloxane) with Hydrophobins for Protein Immobilization, Langmuir 23 (2007) 4465–4471.
[12] T. Lahtinen, M.B. Linder, T. Nakari-Setälä, C. Oker-Blom, Hydrophobin (HFBI): A potential fusion partner for one-step purification of recombinant proteins from insect cells, Protein Expr, Purif. 59 (2008) 18–24, http://dx.doi.org/10.1016/j.pep.2007.12.014.
[13] M. Linder, K. Selber, T. Nakari-seta, The Hydrophobins HFBI and HFBII from *Trichoderma reesei* Showing Efficient Interactions with Nonionic Surfactants in Aqueous Two-Phase Systems, Biomacromolecules. 2 (2001) 511–517.
[14] Z. Wang, Y. Huang, S. Li, H. Xu, M.B. Linder, M. Qiao, Hydrophilic modification of polystyrene with hydrophobin for time-resolved immunofluorometric assay, Biosens. Bioelectron. 26 (2010) 1074–1079, http://dx.doi.org/10.1016/j.bios.2010.08.059.
[15] R. Misra, J. Li, G.C. Cannon, S.E. Morgan, Nanoscale reduction in surface friction of polymer surfaces modified with Sc3 hydrophobin from *Schizophyllum commune*, Biomacromolecules. 7 (2006) 1463–1470, http://dx.doi.org/10.1021/bm050983y.
[16] A.R. Cox, D.L. Aldred, A.B. Russell, Exceptional stability of food foams using class II hydrophobin HFBII, Food Hydrocoll. 23 (2009) 366–376, http://dx.doi.org/10.1016/j.foodhyd.2008.03.001.
[17] T.B.J. Blijdenstein, P.W.N. De Groot, S.D. Stoyanov, On the link between foam coarsening and surface rheology: why hydrophobins are so different, Soft Matter. 6 (2010) 1799–1808, http://dx.doi.org/10.1039/b925648b.
[18] H.K. Valo, H. Laaksonen, L.J. Peltonen, M.B. Linder, J.T. Hirvonen, Multifunctional Hydrophobin: Toward Nanoparticles, ACS Nano 4 (2010) 1750–1758, http://dx.doi.org/10.1021/nn9017558.
[19] H.J. Hektor, K. Scholtmeijer, Hydrophobins: proteins with potential, Curr. Opin. Biotechnol. 16 (2005) 434–439, http://dx.doi.org/10.1016/j.copbio.2005.05.004.
[20] L. Espino-Rammer, D. Ribitsch, A. Przylucka, A. Marold, K.J. Greimel, E.H. Acero, G.M. Guebitz, C.P. Kubicek, I.S. Druzhinina, Two novel class II hydrophobins from Trichoderma spp. Stimulate enzymatic hydrolysis of poly(ethylene terephthalate) when expressed as fusion proteins, Appl. Environ. Microbiol. 79 (2013) 4230–4238, http://dx.doi.org/10.1128/aem.01132-13.
[21] D. Ribitsch, E. Herrero Acero, A. Przylucka, S. Zitzenbacher, A. Marold, C. Gamerith, R. Tscheließnig, A. Jungbauer, H. Rennhofer, H. Lichtenegger, H. Amenitsch, K. Bonazza, C.P. Kubicek, I.S. Druzhinina, G.M. Guebitz, Enhanced cutinase-catalyzed hydrolysis of polyethylene terephthalate by covalent fusion to hydrophobins, Appl. Environ. Microbiol. 81 (2015) 3586–3592, http://dx.doi.org/10.1128/AEM.04111-14.
[22] M. Bailey, S. Askolin, N. Hörhammer, M. Tenkanen, M. Linder, M. Penttilä, T. Nakari-Setälä, Process technological effects of deletion and amplification of hydrophobins I and II in transformants of *Trichoderma reesei*, Appl. Microbiol. Biotechnol. 58 (2002) 721–727, http://dx.doi.org/10.1007/s00253-002-0966-z.
[23] S. Askolin, M. Linder, K. Scholtmeijer, M. Tenkanen, M. Penttilä, M.L. de Vocht, H.A.B. Wösten, Interaction and comparison of a class I hydrophobin from *Schizophyllum commune* and class II Hydrophobins *Trichoderma reesei*, Biomacromolecules 7 (2006) 1295–1301, http://dx.doi.org/10.1021/bm050676s.
[24] C.P. Kurtzman, Biotechnological strains of *Komagataella* (*Pichia*) *pastoris* are *Komagataella phaffii* as determined from multigene, J. Ind. Microbiol. Biotechnol. 36 (2009) 1435–1438, http://dx.doi.org/10.1007/s10295-009-0638-4.
[25] M. Stübner, G. Lutterschmid, R.F. Vogel, L. Niessen, Heterologous expression of the hydrophobin FcHyd5p from *Fusarium culmorum* in *Pichia pastoris* and evaluation of its surface activity and contribution to gushing of carbonated beverages, Int. J. Food Microbiol. 141 (2010) 110–115, http://dx.doi.org/10.1016/j.ijfoodmicro.2010.03.003.
[26] K. Kottmeier, T.J. Günther, J. Weber, S. Kurtz, K. Ostermann, G. Rödel, T. Bley, Constitutive expression of hydrophobin HFB1 from *Trichoderma reesei* in *Pichia pastoris* and its pre-purification by foam separation during cultivation, Eng. Life Sci. 12 (2012) 162–170, http://dx.doi.org/10.1002/elsc.201100155.
[27] B. Niu, D. Wang, Y. Yang, H. Xu, M. Qiao, Heterologous expression and characterization of the hydrophobin HFBI in *Pichia pastoris* and evaluation of its contribution to the food industry, Amino Acids. 43 (2012) 763–771, http://dx.doi.org/10.1007/s00726-011-1126-5.
[28] D. Song, Z. Gao, L. Zhao, X. Wang, H. Xu, Y. Bai, X. Zhang, M.B. Linder, H. Feng, M. Qiao, High-yield fermentation and a novel heat-precipitation purification method for hydrophobin HGFI from *Grifola frondosa* in *Pichia pastoris*, Protein Expr Purif. 128 (2016) 22–28, http://dx.doi.org/10.1016/j.pep.2016.07.014.
[29] W. Li, Y. Gong, H. Xu, M. Qiao, B. Niu, Identification properties of a recombinant class I hydrophobin rHGFI, Int. J. Biol. Macromol. 72 (2015) 658–663, http://dx.doi.org/10.1016/j.ijbiomac.2014.09.014.
[30] A. Lohrasbi-Nejad, M. Torkzadeh-Mahani, S. Hosseinkhani, Heterologous expression of a hydrophobin HFB1 and evaluation of its contribution to producing stable foam, Protein Expr, Purif. 118 (2016) 25–30, http://dx.doi.org/10.1016/j.pep.2015.09.025.
[31] V.K. Morris, M. Sunde, Formation of Amphipathic Amyloid Monolayers from Fungal Hydrophobin Proteins, Protein Nanotechnol. Protoc. Instrum Appl. (2013) 119–129, http://dx.doi.org/10.1007/978-1-62703-354-1.

[32] W. Wohlleben, T. Subkowski, C. Bollschweiler, B. Von Vacano, Recombinantly produced hydrophobins from fungal analogues as highly surface-active performance proteins, Eur. Biophys. J. 39 (2010) 457–468, http://dx.doi.org/10.1007/s00249-009-0430-4.
[33] A. Przylucka, G. Bayram, K. Chenthamara, F. Cai, M. Grujic, J. Karpenko, M. Livoi, Q. Shen, C.P. Kubicek, I.S. Druzhinina, HFB7 −A novel orphan hydrophobin of the Harzianum and Virens clades of Trichoderma, is involved in response to biotic and abiotic stresses, Fungal Genet. Biol. (2017), http://dx.doi.org/10.1016/j.fgb.2017.01.002.
[34] J. Baek, C.M. Kenerley, The *arg2* Gene of *Trichoderma virens*: Cloning and Development of a Homologous Transformation System, Fungal Genet. Biol. 44 (1998) 34–44.
[35] F. Ausubel, R. Brent, R.E. Kingston, D.D. Moore, J.G. Seidman, J.A. Smith, K. Struhl, One-Dimensional SDS Gel Electrophoresis of Proteins, Curr. Protoc, Mol. Biol. 2A (2003) 4, p. Unit 10.
[36] R. Gundry, M.Y. White, C.I. Murray, L.A. Kane, Q. Fu, B.A. Stanley, J.E. Van Eyk, Preparation of Proteins and Peptides for Mass Spectrometry Analysis in a Bottom-Up Proteomics Workflow, in, Curr. Protoc. Mol. Biol. (2009), p. Unit10.25.
[37] C. Louis-Jeune, M.A. Andrade-Navarro, C. Iratxeta, Derived spectra, Proteins 80 (2011) 374–381, http://dx.doi.org/10.1002/prot.23188.
[38] C. Wiedemann, P. Bellstedt, M. Go, Structural bioinformatics CAPITO—a web server-based analysis and plotting tool for circular dichroism data, Bioinformatics. 29 (2013) 1750–1757, http://dx.doi.org/10.1093/bioinformatics/btt278.
[39] A. Sali, T.L. Blundell, Comparative protein modelling by satisfaction of spatial restraints, J. Mol. Biol. 234 (1993) 779–815.
[40] K. Bonazza, R. Gaderer, S. Neudl, A. Przylucka, G. Allmaier, I.S. Druzhinina, The fungal cerato-platanin protein EPL1 forms highly ordered layers at hydrophobic/hydrophilic interfaces, Soft Matter. 11 (2015) 1723–1732, http://dx.doi.org/10.1039/C4SM02389G.
[41] B.O. Keller, J. Sui, A.B. Young, R.M. Whittal, Interferences and contaminants encountered in modern mass spectrometry, Anal. Chim. Acta. 627 (2008) 71–81.
[42] J. Hakanpää, A. Paananen, S. Askolin, T. Nakari-Setälä, T. Parkkinen, M. Penttilä, M.B. Linder, J. Rouvinen, Atomic Resolution Structure of the HFBII Hydrophobin, a Self-assembling Amphiphile, J. Biol. Chem. 279 (2004) 534–539, http://dx.doi.org/10.1074/jbc.M309650200.
[43] J. Hakanpää, G.R. Szilvay, H. Kaljunen, M. Maksimainen, M. Linder, J. Rouvinen, Two crystal structures of Trichoderma reesei hydrophobin HFBI-the structure of a protein amphiphile with and without detergent interaction, Protein Sci 15 (2006) 2129–2140, http://dx.doi.org/10.1110/ps.062326706.
[44] V.N. Uversky, Natively unfolded proteins: A point where biology waits for physics, Protein Sci. 11 (2002) 739–756.
[45] H. Fan, X. Wang, J. Zhu, G.T. Robillard, A.E. Mark, Molecular dynamics simulations of the hydrophobin SC3 at a hydrophobic/hydrophilic interface, Proteins 64 (2006) 863–873.
[46] T. Neuhof, R. Dieckmann, I.S. Druzhinina, C.P. Kubicek, T. Nakari-seta, H. Von Do, Direct identification of hydrophobins and their processing in Trichoderma using intact-cell MALDI-TOF MS, FEBS J 274 (2007) 841–852, http://dx.doi.org/10.1111/j.1742-4658.2007.05636.x.
[47] M. Mikus, L. Hatvani, T. Neuhof, M. Komon-Zelazowska, R. Dieckmann, T. Schwecke, I.S. Druzhinina, H. von Döhren, C.P. Kubicek, Differential regulation and posttranslational processing of the class II hydrophobin genes from the biocontrol fungus *Hypocrea atroviridis*, Appl. Environ. Microbiol. 75 (2009) 3222–3229.
[48] J. Arié, M. Miot, N. Sassoon, J. Betton, Formation of active inclusion bodies in the periplasm of Escherichia coli, Mol. Microbiol. 62 (2006) 427–437, http://dx.doi.org/10.1111/j.1365-2958.2006.05394.x.
[50] M.L. de Vocht, I. Reviakine, H.A. Wosten, A. Brisson, J.G. Wessels, G.T. Robillard, Structural and functional role of the disulfide bridges in the hydrophobin SC3, J Biol Chem. 275 (2000) 28428–28432, http://dx.doi.org/10.1074/jbc.M000691200.
[51] Q. Ren, A.H. Kwan, M. Sunde, Solution structure and interface-driven self-assembly of NC2, a new member of the Class II hydrophobin proteins, Proteins. 82 (6) (2014) 990–1003, http://dx.doi.org/10.1002/prot.24473.
[52] I. Gall, M. Herzberg, Y. Oren, The effect of electric fields on bacterial attachment to conductive surfaces, Soft Matter. 9 (2013) 2443–2452.
[53] C. Fredriksson, S. Kihlman, M. Rodahl, B.H. Kasemo, The Piezoelectric Quartz Crystal Mass and Dissipation Sensor: A Means of Studying Cell Adhesion, Langmuir 14 (1998) 248–251.
[54] I.M. Tucker, J.T. Petkov, J. Penfold, R.K. Thomas, A.R. Cox, N. Hedges, Adsorption of hydrophobin-protein mixtures at the air-water interface: The impact of ph and electrolyte, Langmuir. 31 (2015) 10008–10016, http://dx.doi.org/10.1021/acs.langmuir.5b02403.
[55] M. Linder, G.R. Szilvay, H. So, Surface adhesion of fusion proteins containing the hydrophobins HFBI and HFBII from *Trichoderma reesei*, Protein Sci. 11 (2002) 2257–2266, http://dx.doi.org/10.1110/ps.0207902, bonding.
[56] Y. Corvis, A. Walcarius, R. Rink, N.T. Mrabet, E. Rogalska, Preparing Catalytic Surfaces for Sensing Applications by Immobilizing Enzymes via Hydrophobin Layers, Anal. Chem. 77 (2005) 1622–1630, http://dx.doi.org/10.1021/ac048897w.
[57] R. Bilewicz, J. Witomski, A. Van der Heyden, D. Tagu, B. Palin, E. Rogalska, Modification of electrodes with self-assembled hydrophobin layers, J. Phys. Chem. B. 105 (2001) 9772–9777, http://dx.doi.org/10.1021/jp0113782.
[58] H. Valo, M. Kovalainen, P. Laaksonen, M. Häkkinen, S. Auriola, L. Peltonen, M. Linder, K. Järvinen, J. Hirvonen, T. Laaksonen, Immobilization of protein-coated drug nanoparticles in nanofibrillar cellulose matrices-Enhanced stability and release, J. Controlled Release. 156 (2011) 390–397, http://dx.doi.org/10.1016/j.jconrel.2011.07.016.
[59] U. Weickert, F. Wiesend, T. Subkowski, A. Eickhoff, G. Reiss, Optimizing biliary stent patency by coating with hydrophobin alone or hydrophobin and antibiotics or heparin: an *in vitro* proof of principle study, Adv. Med. Sci. 56 (2011) 138–144, http://dx.doi.org/10.2478/v10039-011-0026-y.
[60] M.I. Janssen, M.B.M. Van Leeuwen, T.G. Van Kooten, J. De Vries, L. Dijkhuizen, H.A.B. Wösten, Promotion of fibroblast activity by coating with hydrophobins in theβ-sheet end state, Biomaterials 25 (2004) 2731–2739, http://dx.doi.org/10.1016/j.biomaterials.2003.09.060.